Visualization and Processing of Structural Monitoring Data Using Space-Time Cubes

Luigi Barazzetti[1], Mattia Previtali[1(✉)], and Fabio Roncoroni[2]

[1] Department of Architecture, Built Environment and Construction Engineering, Politecnico di Milano, Piazza Leonardo da Vinci 32, Milan, Italy
{luigi.barazzetti,mattia.previtali}@polimi.it
[2] Polo territoriale di Lecco, via Previati 1/c, Lecco, Italy
fabio.roncoroni@polimi.it

Abstract. This paper aims to analyze space-time cubes for visualizing and processing multi-temporal spatial monitoring data. The proposed case study is the Cathedral of Milan (Duomo di Milano), which has a set of monitoring time series spanning more than half a century. Differential vertical movements are periodically measured for the cathedral columns, constituting a continuous spatio-temporal dataset for structural health monitoring. More specifically, the space time pattern mining toolbox in ArcGIS Pro was used to (i) create a space-time cube and (ii) perform advanced analysis using the monitoring dataset, including time-series clustering and forecasting operations.

Keywords: GIS · Monitoring · Space time cube · Time series

1 Introduction

Visualization and processing of multiple time-series associated with different georeferenced entities is a complex task requiring spatio-temporal algorithms and representation techniques. The dataset considered in this paper is a time-series collection of relative elevation values $Z_{t,i}$ measured by high precision geometric leveling. The considered points are monitoring benchmarks mounted on 59 pillars (index $i = 1, ..., 59$) of the Cathedral of Milan (Duomo di Milano), the Gothic masterpiece symbol of the city [1,2]. The spatial location (X_i, Y_i) of the columns is known and constant over time. In contrast, the elevation value $Z_{t,i}$ is the monitored parameter and represents the movement caused by subsidence.

Structural monitoring in the Cathedral of Milan using high precision geometric leveling started during the '60s, when the extraction of water from the ground in the city produced a rapid drop of the water table, resulting in differential vertical movements of the pillars and structural instability [3,4].

This paper does not describe other monitoring systems installed in the Cathedral, including both static and dynamic methods. The reader is referred to [5–7]

© The Author(s), under exclusive license to Springer Nature Switzerland AG 2022
O. Gervasi et al. (Eds.): ICCSA 2022, LNCS 13376, pp. 19–31, 2022.
https://doi.org/10.1007/978-3-031-10450-3_2

for some examples. This paper aims to use space-time cubes to visualize and process time-series of vertical differential measurements, which are periodically calculated from elevation values derived by geometric leveling operations (Fig. 1). Least squares adjustment is used to obtain elevations with a precision of about ±0.1 mm, which is sufficient to track the movements over time.

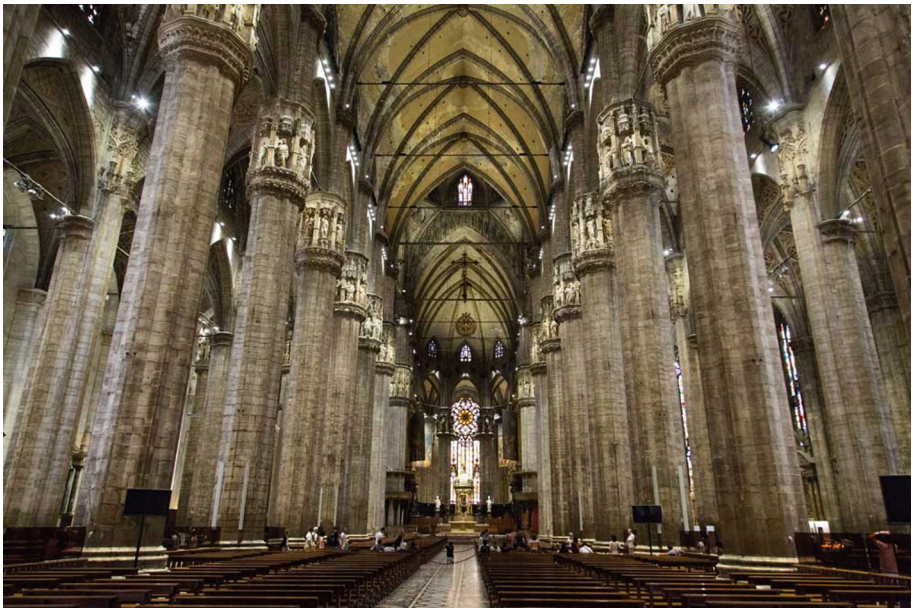


Fig. 1. View of the pillars along the nave, the picture was acquired close to the central entrance of the cathedral.

Analysis and interpretation of monitoring time-series require efficient methods to provide facilitated access and visualization and support for data analytics, mainly when multiple spatio-temporal sequences are simultaneously used. Indeed, plotting in a single graph the data acquired for the different 59 locations (i.e., the columns of the Cathedral) provides a confusing representation and loses the spatial relationship between the columns.

The displacement of a column must be analyzed using an approach that considers the spatial position and the relationships with other columns. The monument comprises several interconnected structural elements (foundations, pillars, arches, vaults, tie-rods, etc.) with mutual interaction. The opportunity to simultaneously visualize monitoring data considering both spatial and temporal aspects is attractive and opens new possibilities to understand better structural behavior.

The idea is to use methods able to combine time series available as triplets $(X_i, Y_i, Z_{t,i})$ acquired overtime using an advanced representation with fixed spatial locations. In contrast, the third dimension corresponds to the variable's values at different times, which are adjusted elevation and their variations.

As mentioned, the problem faced in this paper is to exploit a space-time cube (STC) featuring both spatial and temporal structures. Space-time cubes became more popular in the last decade and emerged in connection with Big Data analysis and applications like weblogs, sensor networks, and cloud computing. In particular, the concept of space-time cube (also named hyper-cubes) was introduced in Business Intelligence to implement Data Dashboard and Data Warehouse concepts. The term "cube" is used in Business Intelligence to address a multidimensional data set. In database engineering and computer science, an OLAP (Online Analytical Processing) cube refers to a multidimensional array of data [8] that can be processed online [9]. In addition, Data-Cube structures gained significant attention recently for satellite imagery management and spatial data analytic domain. Examples of application domain for space-time cube are, among other, analysis of spatio-temporal pattern for COVID-19 spread [10], distribution of extreme weather events [11], modelling crime patterns in urban areas [12], road traffic and crash analysis [13]. A review of temporal data visualization based on space-time cubes (including different operations such as extracting sub-parts, flattening across space or time, and transforming the cube's geometry) is described in [14,15].

The work described in this paper was carried out with ArcGIS Pro v.2.9, which allows the creation and analysis of space-time cubes. The cube has rows, columns, and time steps, which correspond to X, Y, and Z coordinates, as shown in Fig. 2.

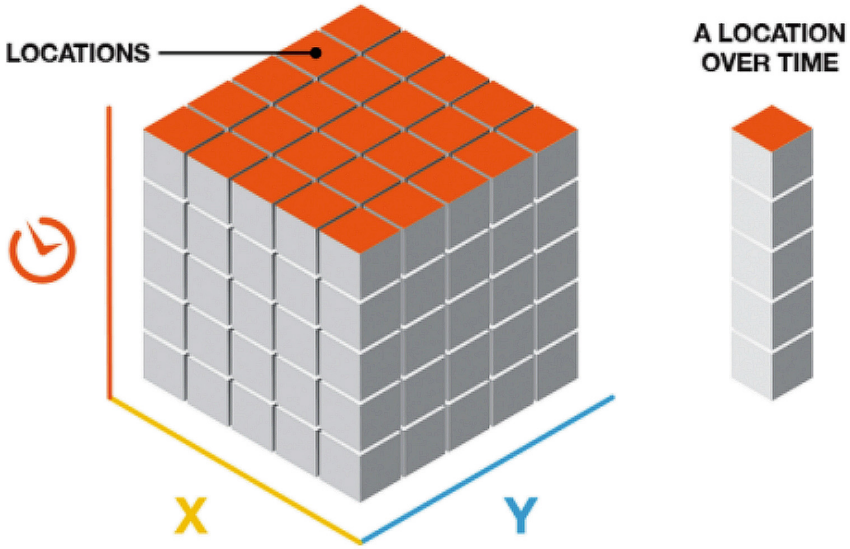


Fig. 2. Structure of the space-time cube, figure retrieved form https://pro.arcgis.com/.

The cube is saved using the Network Common Data Format (NetCDF), which is "a set of software libraries and self-describing, machine-independent data formats that support the creation, access, and sharing of array-oriented scientific data. The climate and forecast (CF) metadata conventions are designed to promote the processing and sharing of netCDF files", as described in www.ogc.org/standards/netcdf.

2 Creation of the Space-Time Cube

2.1 Data Description

The dataset used in this paper is a geometric leveling time-series collection acquired in the Cathedral of Milan. The installation of a geometric leveling monitoring network began in 1961 to track differential vertical movements induced by subsidence caused by water extraction from the ground.

The actual configuration of the leveling network still preserves continuity with original measurements. Benchmarks are installed on 59 pillars along the nave, the transept, and the apse. The frequency of data acquisition is based on two measurement campaigns in a year, in May and November. Readings are carried out with a high-precision level, and network geometry follows a rigid scheme with multiple closed loops with self-intersections. After completing a closed circuit, the misclosure (which should be theoretically zero) is compared to the tolerance c, which is estimated as $c = \pm 0.1\sqrt{n}$ mm, where n is the number of benchmarks in a closed loop. As the distance between the benchmarks is relatively short and rather constant, the distance is not considered in calculating the tolerance, which only depends on the number of points.

The acquired data (a redundant set of height differences) are adjusted using least squares, obtaining elevation values and their precision, which is in the order of ± 0.1 mm. The data set in this paper is based on the relative vertical displacements measured between May 1970 and November 2020, i.e., a period of about 50 years. Data are also available for a more extended period (back to 1965). However, the configuration used today is still based on the 1969 configuration. For this reason, the dataset presented in this paper starts from May 1970.

2.2 Creation and Visualization of the Space-Time Cube in 3D

Monitoring data are structured into tables reporting variations in elevation computed considering column n. 39 as fixed. The benchmark installed on this column is the historical reference for all measurements (i.e., its height is assumed as constant over time). This choice is motivated by the need for the monitoring project. It is impossible to find a stable reference point in the area because subsidence affects the cathedral and the surrounding buildings. For this reason, pillar 39 was chosen as a reference to capture differential vertical movements, i.e., those movements that could impact the stability of the cathedral.

The spatial location of the columns is known and stored in a point feature layer, allowing the creation of a spatio-temporal dataset. The reference system

for planar coordinates is UTM-WGS84 32N, thus data are available as $East = X$ and $North = Y$ using metric units in meters. Vertical movements are instead reported in millimeters and can be estimated as $\Delta z_{t,i} = H_{t,i} - H_{1970,i}$, where H_i is the adjusted elevation using least squares, and index i refers to the pillar number. After importing the data in ArcGIS Pro, the reference system was changed to WGS1984 Web Mercator (Auxiliary Sphere).

The creation of the space-time cube was carried out using version 2.9. As mentioned, the point feature layer was used to define the spatial location of pillars with benchmarks. An one-to-many relationship was created to relate the point feature to a table with the measured variations $\Delta z_{t,i}$ and the corresponding date. The chosen time-step interval is six months and covers May 1970–November 2020.

The STC was generated without aggregation so that the different elements include the adjusted coordinates (Fig. 3). Color variation (from white to purple) along Z depends on the magnitude of differential movements. The interface provides facilitated access to specific data. For instance, selecting an element of the STC provides information about the pillar number and the measured variation at a particular time.

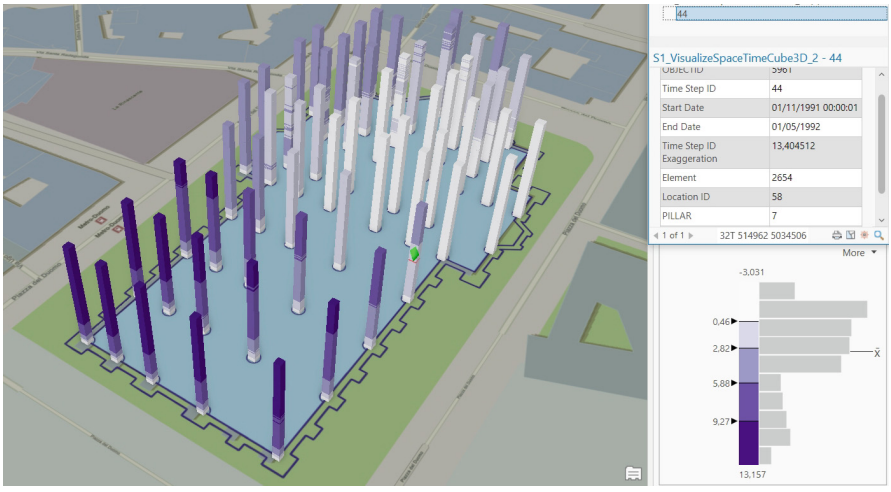


Fig. 3. The space-time cube encapsulating monitoring measurements. (Color figure online)

The space-time cube also has an associated attribute table, which can be used for queries. For instance, the user can visualize (in 3D) those time steps for all pillars with relative movements larger than a specif threshold or limit the query to just a subset of columns. Such options are useful when used together with other layers, which can be exploited to classify the pillars with additional information. For instance, columns can be grouped depending on their specific location inside the cathedral (i.e., nave, transept, apse, ...).

The time series collection can also be visualized using graphs. Figure 4 shows a chart created using data from pillars 74-75-84-85, i.e., the pillars of the tiburium, under the main spire (Guglia Maggiore) of the Duomo. Charts are not static representations, but they can be interactively inspected in ArcGIS Pro, and eventually exported. Query definition also applies to charts.

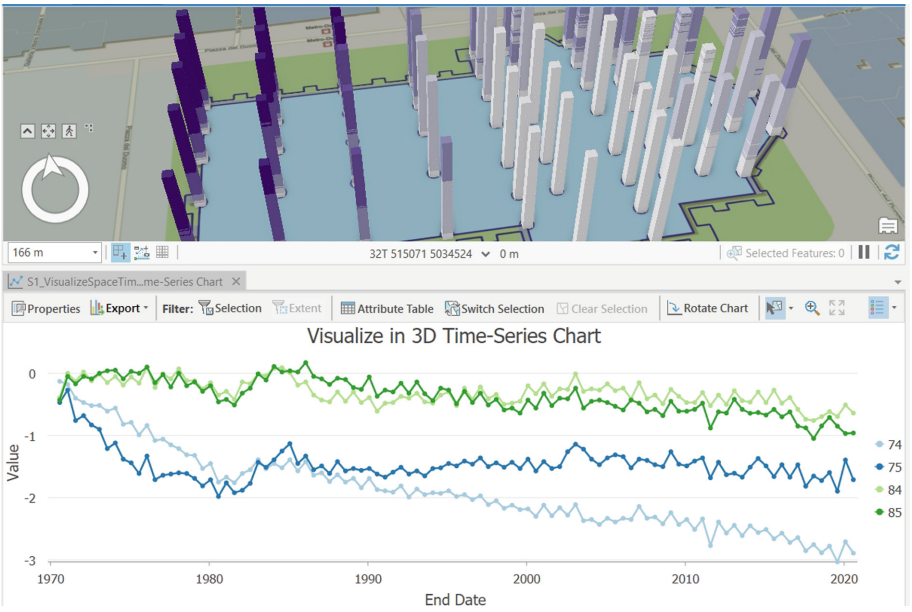


Fig. 4. Charts for the pillars of the tiburium generated using the STC.

The space-time cube can also be visualized in 2D, i.e., with a traditional planar cartographic visualization. Figure 5 shows the space-time cube with a color representation depending on the detected trends. As pillar n. 39 has always been chosen as a reference to compute differential displacements, movements are both positive (up) and negative (down). As can be seen, points 39 shows no significant trend. Pillars 88, 75, and 43 also have no significant trends, meaning that their movements tend to become constant over time. Instead, pillars of the apse and the nave have a positive trend, notwithstanding the magnitude cannot be quantified using such representation. Finally, a significant part of the transept shows a negative trend, indicating that the movements are the opposite if compared to the nave and facade. Additional results can be obtained using the created space-time cube. The next sections will illustrate some other operations that can be carried out to understand the differential movements better.



Fig. 5. Visualization of the trend related to different vertical movements (up or down) using pillar 39 as a fixed reference.

3 Time Series Clustering

Time-series clustering is the task of creating time-series groups depending on similarity parameters. Different options are available in ArcGIS Pro and Fig. 6 shows the results using two different methods: clustering based on the $\Delta z_{t,i}$ values and clustering based on correlation. The method based on the values compares $\Delta z_{t,i}$ magnitude, whereas clustering based on correlation determines if the time-series are correlated across time. Processing was done selecting 4 classes.

The two results can be interpreted as follows. In the case of clustering based on the value, a cluster is created for the pillars in the southern part of the transept (green). This area is historically the one characterized by maximum lowering. A second cluster (light green) is created around this area, which is surrounded by the pillars clustered in yellow mainly located on the apse, the northern part of the transept, and half of the nave. The last cluster (dark green) is mainly concentrated in the second half of the nave towards the facade.

Such a result can be compared with a visualization based on the interpolated surface of differential movements in the period 1970–2020 (Fig. 7). An interpolation based on rational basis splines was carried out to obtain a continuous representation from punctual data. Then, the grid model was represented with a similar color map used for the classification. The number of classes chosen is higher to better perceive the variations, so that colours of Figs. 6 and 7 do not match. However, they depict a similar trend in the value, indicating that the area with maximum negative displacement is the transept, whereas the largest positive values are in the area of the facade, especially in the North-West corner.

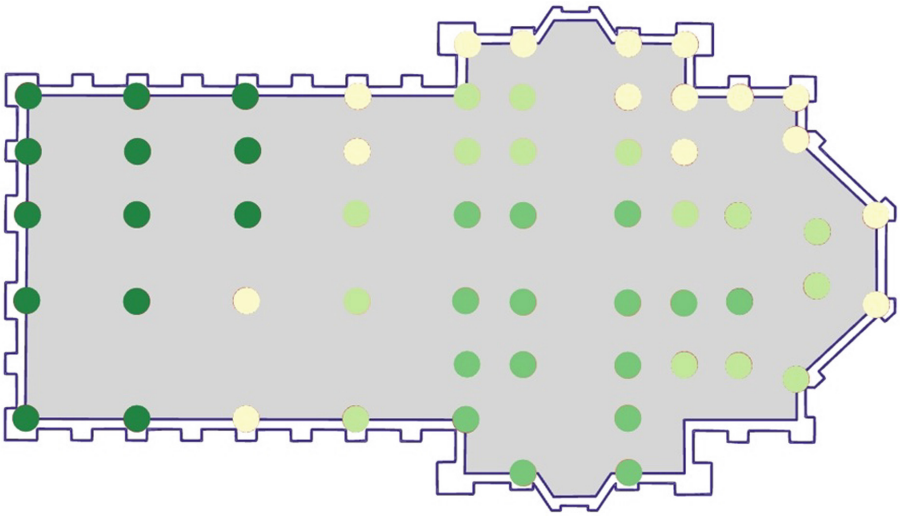


Fig. 6. Clustering based on $\Delta z_{t,i}$ values. (Color figure online)

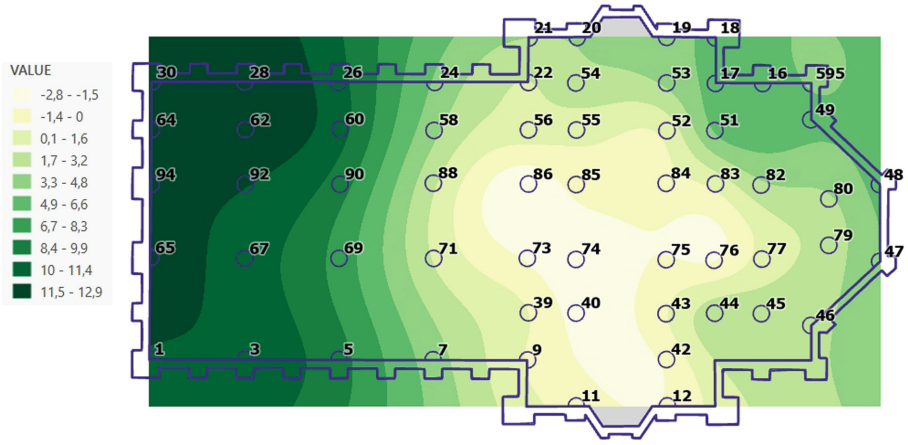


Fig. 7. Interpolated displacement map generated using rational basis functions. (Color figure online)

Figure 8 shows clustering results based on the correlation. The number of chosen classes is still 4. In this case, the achieved result shows groups of columns tending to increase (or decrease) in a similar way.

Column 39 forms a class because it is the only column with constant zero value. A second class (orange) is composed of columns mainly located in the southern part of the transept, including the 4 main columns of the tiburium that are located in the middle of the transept. The third class (rose) is made

up of columns mainly located around those pillars in the second class. The last class (red) includes columns of the nave and the apse.

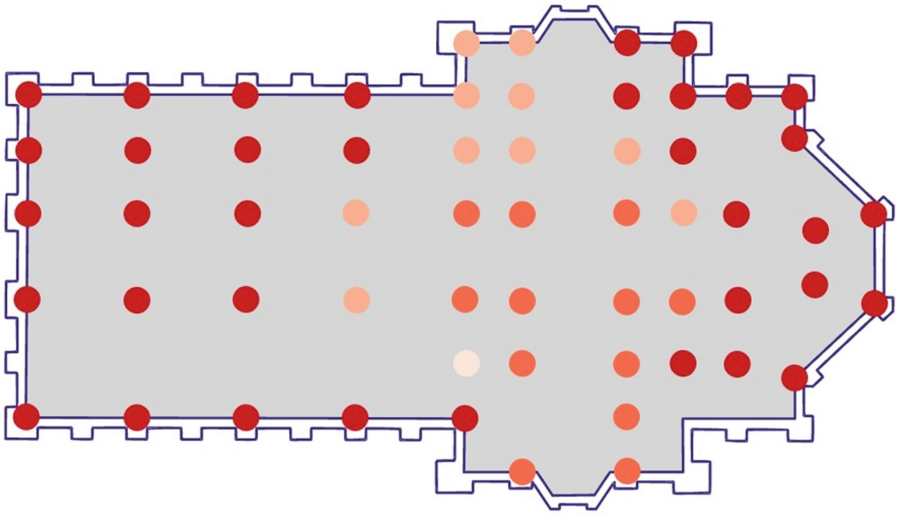


Fig. 8. Clustering results based on correlation. (Color figure online)

4 Time Series Forecast

Forecasting future values is one of the methods to find discontinuities in time series. A basic detection method could be based on forecasting the value at $t+1$ given the previously measured values at time $1, ..., t$. If the measured value at epoch $t+1$ is significantly larger than the forecast value (considering the precision of measurements, which is ± 0.1 mm in this case, and the forecast quality), the considered column could deserve more attention. In this way, a threshold could be set to identify anomalous variations.

Different options are available to perform time series forecasting using the space-time cube created in Arcgis Pro. The first option is based on curve fitting methods, which are used to interpolate the data using a specific function and then estimate future values. ArcGIS Pro offers different models: linear, parabolic, exponential, and S-shaped (using a Gompertz curve). All estimation methods can also be simultaneously run on the STC. An automatic selection of the best result is carried out using the validation root mean square error (RMSE), which is calculated on selected final time steps previously excluded during the fitting phase. The computed model is then evaluated at those time steps. The RMSE is equal to the square root of the average squared difference between the forecasted and original values of the excluded time step.

However, such methods were not used in this work because most of the time series do not follow those models, as it can be verified with a simple plotting and visual check of the time series.

The second method available in ArcGIS Pro is based on forecasting using the Holt-Winters exponential smoothing method. This algorithm decomposes the time series at each location cube into seasonal and trend components, assuming the seasonal behavior and the trend can be separated. Also in this case, this assumption does not always hold for the different time-series in the STC.

The third method is a forest-based forecast, which uses an adaptation of Leo Breiman's random forest algorithm. The method is suitable to model complicated shapes and trends, which are instead challenging to handle with predefined mathematical functions. It also requires fewer initial assumptions than the Holt-Winters exponential smoothing method.

Figure 9 shows some results achieved with such method, using the observation in the period 1970–2014 for training and 2015–2020 as validation. The considered columns are n. 40 (top) and n. 55 (bottom) notwithstanding, forecasting is carried out for the whole dataset.

No outlier detection was applied because all the time series come from already adjusted data (elevation values), in which methods to identify outliers are integrated. The used forecasting algorithm builds the model by values after detrending, i.e., values within the time window are linearly detrended, and the dependent variable is represented by its detrended value.

The statistics on the training dataset provided an average RMS of 0.05 mm and a standard deviation of ±0.01 mm. The RMS on the validation dataset gave an average of 0.27 mm and a standard deviation of ±0.015 mm. This last value is not significantly different from the evaluation precision achieved after Least Squares adjustment.

The forecasted value considers two additional time steps, i.e., the measurements for May and November 2021. Therefore, forecasting was carried out for the year 2021.

Statistics are also available for individual time series. In the case of column n. 40, the validation RMS is ±0.09 mm, whereas column n. 55 shows a larger validation RMS of ±0.21 mm. The method is also able to estimate a level of confidence for the forecasted value, which is illustrated at 90% in Fig. 9. As can be seen, the confidence level is different for the two time-series here proposed because the second one has a more irregular behavior.

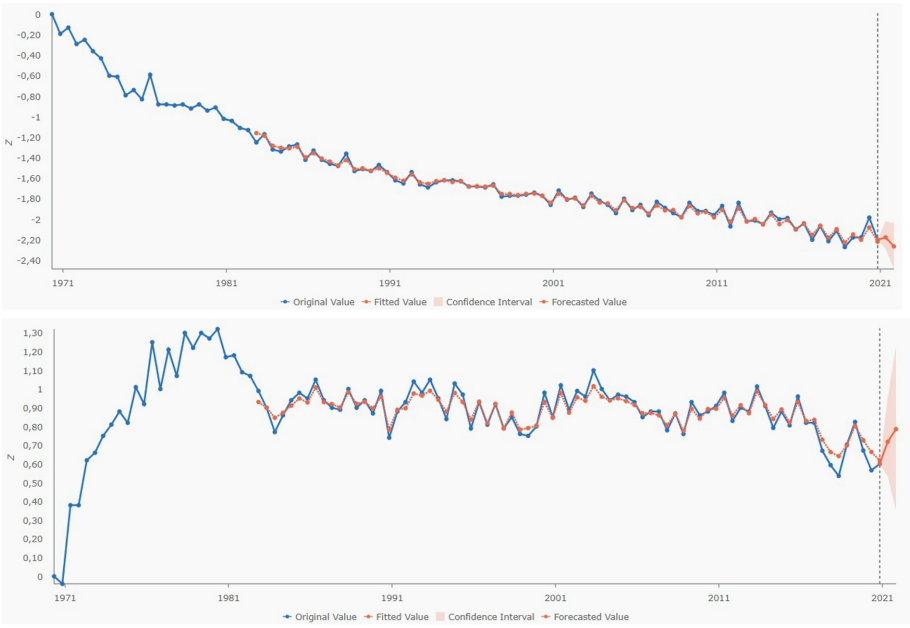


Fig. 9. Results after time-series forecasting for columns n. 40 (top) and n. 55 (bottom).

5 Conclusions

Efficient storage and visualization are essential in structural monitoring applications. The proposed work started from an important consideration: the monitoring system of vertical movements of the Cathedral of Milan is particularly suitable for a GIS-based representation. Displacements of vertical movements are measured using a set of benchmarks installed on the columns; therefore, a space-time cube is an attractive opportunity to combine X, Y cartographic coordinates and vertical variations measured over time.

After creating the STC, additional processing using all the time series was carried out. Clustering algorithms allowed the creation of groups of columns with similar movements, using both the values of the measured displacements and the correlation between time series. Forecasting is helpful to predict future values and verify if newly measured displacements are similar to forecasted values, i.e., establishing an alternative method to detect anomalous values. Therefore, such a method is considered an integration of the traditional work carried out in the Duomo.

Future work will consider the use of interpolated data in other specific locations. Interpolated maps of displacements (such as the one in Fig. 7) provide information about the whole Cathedral. As the STC also supports multidimensional raster datasets, creating a STC not limited to the measured values seems

an interesting opportunity. The aim will be the extension of the analysis to the whole Cathedral.

Acknowledgments. The work is carried our within the framework of the collaboration between Veneranda Fabrica del Duomo di Milano and Politecnico di Milano. The authours want to thank Francesco Canali, director of Cantieri del Duomo di Milano for the Veneranda Fabbrica del Duomo.

References

1. Ferrari da Passano, C.: Il Duomo rinato: Storia e tecnica del restauro statico dei piloni del tiburio del Duomo di Milano. Veneranda Fabbrica del Duomo (Diakronia), Milan (1988). (in Italian)
2. Ferrari da Passano, C.: La Gran Guglia, il Duomo e l'acqua. Una piccola storia sulle vicissitudini e i misteri lungo i secoli ed i loro strani rapporti (2019). Puslihed online in Dicember 2019. http://www.risorsa-acqua.it/tag/ferrari-da-passano/
3. Croce, A.: Questioni geootecniche sulle fondazioni del Duomo di Milano. In: Il Duomo rinato: Storia e tecnica del restauro statico dei piloni del tiburio del Duomo di Milano, vol. 2 (1970)
4. Barazzetti, L., Roncoroni, F.: Relazione sulle misure eseguite per il controllo delle deformazioni del Duomo di Milano. Semestral report for the Veneranda Fabrica del Duomo di Milano, 39 p. (2020)
5. Alba, M., Roncoroni, F., Barazzetti, L., Giussani, A., Scaioni, M.: Monitoring of the main spire of the Duomo di Milano. In: Joint International Symposium on Deformation Monitoring, Hong Kong, China, 2–4 November 2011, 6 p. (2011)
6. Cigada, A., Dell'Acqua, L., Castiglione, B., Scaccabarozzi, M., Vanali, M., Zappa, E.: Structural health monitoring of an historical building: the main spire of the Duomo Di Milano. Int. J. Archit. Herit. **11**(4), 501–518 (2016)
7. Barazzetti, L., Canali, F., Della Torre, S., Previtali, M., Roncoroni, F.: Monitoring the Cathedral of Milan: An Archive with More Than 50 Years of Measurements. Lecture Notes in Computer Sciences, 16 p. (2021). in press
8. Gray, J., Bosworth, A., Layman, A., Pirahesh, H.: Data cube: a relational aggregation operator generalizing group-by, cross-tab, and sub-totals. In: Proceedings of the International Conference on Data Engineering (ICDE), pp. 152–159 (1996)
9. Dubler, C., Wilcox, C.: Just what are cubes anyway? A painless introduction to OLAP technology (2002). https://docs.microsoft.com/. Accessed Feb 2022
10. Mo, C., et al.: An analysis of spatiotemporal pattern for COIVD-19 in China based on space-time cube. J. Med. Virol. **92**(9), 1587–1595 (2020)
11. Allen, M.J., Allen, T.R., Davis, C., McLeod, G.: Exploring spatial patterns of Virginia Tornadoes using kernel density and space-time cube analysis (1960–2019). ISPRS Int. J. Geo Inf. **10**(5), 310 (2021)
12. Hashim, H., Wan Mohd, W.M.N., Sadek, E.S.S.M., Dimyati, K.M.: Modeling urban crime patterns using spatial space time and regression analysis. In: International Archives of the Photogrammetry, Remote Sensing Spatial Information Sciences (2019)
13. Wu, P., Meng, X., Song, L.: Identification and spatiotemporal evolution analysis of high-risk crash spots in urban roads at the microzone-level: using the space-time cube method. J. Transp. Saf. Secur. 1–21 (2021). https://doi.org/10.1080/19439962.2021.1938323

14. Bach, B., Dragicevic, P., Archambault, D., Hurter, C., Carpendale, S.: A descriptive framework for temporal data visualizations based on generalized space-time cubes. In: Computer Graphics Forum, vol. 36, no. 6, pp. 36–61 (2017)
15. Bach, B., Dragicevic, P., Archambault, D., Hurter, C., Carpendale, S.: A review of temporal data visualizations based on space-time cube operations. In: Eurographics Conference on Visualization (EuroVis 2014), pp. 23–41 (2014)